BJP British Journal of Pharmacology

DOI:10.1111/bph.12441
www.brjpharmacol.org

RESEARCH PAPER

G protein-gated inwardly rectifying potassium ($K_{IR}3$) channels play a primary role in the antinociceptive effect of oxycodone, but not morphine, at supraspinal sites

Atsushi Nakamura[1,2], Masahide Fujita[1], Hiroko Ono[1], Yoshie Hongo[1], Tomoe Kanbara[1,2], Koichi Ogawa[1], Yasuhide Morioka[1], Atsushi Nishiyori[1], Masahiro Shibasaki[2], Tomohisa Mori[2], Tsutomu Suzuki[2], Gaku Sakaguchi[1], Akira Kato[1] and Minoru Hasegawa[1]

[1]*Pain & Neurology, Medicinal Research Laboratories, Shionogi Co., Ltd., Osaka, Japan, and* [2]*Department of Toxicology, Hoshi University School of Pharmacy and Pharmaceutical Sciences, Tokyo, Japan*

Correspondence
Minoru Hasegawa, Pain & Neurology, Medicinal Research Laboratories, Shionogi & Co., Ltd, 1-1, 3-chome, Futaba-cho, Toyonaka, Osaka 561-0825, Japan. E-mail: minoru_hasegawa@shionogi.co.jp

Atsushi Nakamura and Masahide Fujita contributed equally to this work.

Keywords
oxycodone; morphine; antinociception; μ-opioid receptor; G protein-gated inwardly rectifying potassium channel

Received
12 July 2013
Revised
17 September 2013
Accepted
25 September 2013

BACKGROUND AND PURPOSE
Oxycodone and morphine are μ-opioid receptor agonists prescribed to control moderate-to-severe pain. Previous studies suggested that these opioids exhibit different analgesic profiles. We hypothesized that distinct mechanisms mediate the differential effects of these two opioids and investigated the role of G protein-gated inwardly rectifying potassium ($K_{IR}3$ also known as GIRK) channels in their antinociceptive effects.

EXPERIMENTAL APPROACH
Opioid-induced antinociceptive effects were assessed in mice, using the tail-flick test, by i.c.v. and intrathecal (i.t.) administration of morphine and oxycodone, alone and following inhibition of $K_{IR}3.1$ channels with tertiapin-Q (30 pmol per mouse, i.c.v. and i.t.) and $K_{IR}3.1$-specific siRNA. The antinociceptive effects of oxycodone and morphine were also examined after tertiapin-Q administration in the mouse femur bone cancer and neuropathic pain models.

KEY RESULTS
The antinociceptive effects of oxycodone, after both i.c.v. and i.t. administrations, were markedly attenuated by $K_{IR}3.1$ channel inhibition. In contrast, the antinociceptive effects of i.c.v. morphine were unaffected, whereas those induced by i.t. morphine were attenuated, by $K_{IR}3.1$ channel inhibition. In the two chronic pain models, the antinociceptive effects of s.c. oxycodone, but not morphine, were inhibited by supraspinal administration of tertiapin-Q.

CONCLUSION AND IMPLICATIONS
These results demonstrate that $K_{IR}3.1$ channels play a primary role in the antinociceptive effects of oxycodone, but not those of morphine, at supraspinal sites and suggest that supraspinal $K_{IR}3.1$ channels are responsible for the unique analgesic profile of oxycodone.

Abbreviations
FBC, femur bone cancer; LH, luria broth; $K_{IR}3$, G protein-gated inwardly rectifying potassium; i.t., intrathecal; MPE, maximal possible effect; PTX, pertussis toxin

Introduction

Morphine and oxycodone are clinically prescribed μ-opioid receptor agonists that control moderate-to-severe pain. Although both opioids show potent analgesic effects against various types of pain (Moulin *et al.*, 1996), they have different analgesic profiles (Koyyalagunta *et al.*, 2012). For example, oxycodone has been reported in some cases to control cancer pain more effectively than morphine (Heiskanen and Kalso, 1997; Mercadante and Arcuri, 1998; Watson and Babul, 1998; Portenoy *et al.*, 1999; Bercovitch and Adunsky, 2006; Silvestri *et al.*, 2008). It is also known that switching from one opioid to another, commonly referred to as 'opioid rotation', often provides improved pain management, suggesting that the underlying analgesic mechanisms of oxycodone and morphine differ.

Both morphine and oxycodone produce analgesic effects by specifically acting on μ-opioid receptors, and *in vitro* experiments have demonstrated that oxycodone has lower agonist activity at μ-opioid receptors than morphine in the rodent spinal cord and brain (Lemberg *et al.*, 2006; Narita *et al.*, 2008). However, when these two opioids are s.c. administered, oxycodone shows equivalent or even more potent analgesic effects than morphine. One possible explanation for this paradoxical effect, in which the *in vitro* potency profiles do not reflect *in vivo* analgesic potencies, is a difference in the pharmacokinetics between the two opioids. Morphine and oxycodone are thought to exert their analgesic effects by acting on μ-opioid receptor in the CNS, and oxycodone passes through the blood–brain barrier more actively than morphine (Tunblad *et al.*, 2003; Bostrom *et al.*, 2006; 2008). Thus, different pharmacokinetic profiles in the CNS appear to account, at least in part, for the characteristic greater analgesic potency of oxycodone compared with morphine after systemic administration. This paradoxical effect has also been observed with local opioid administration into supraspinal sites. When oxycodone and morphine were applied by i.c.v. administration, oxycodone showed similar analgesic potency to morphine despite its weaker *in vitro* potency profile. These results suggest that the mechanisms underlying the antinociceptive effects at supraspinal sites differ between the two μ-opioid receptor agonists.

Multiple mechanisms mediate the opioid analgesic effect, including inhibition of voltage-gated Ca^{2+} channels, activation of voltage-gated potassium channels and activation of the G protein-gated inwardly rectifying potassium ($K_{IR}3$ or GIRK) channels (Yoshimura and North, 1983; Vaughan *et al.*, 1997). Among these, the $K_{IR}3$ channels are directly activated by G proteins that act as important mediators of the morphine-induced analgesic effect at the spinal level (Marker *et al.*, 2002; 2004). However, little is known about the role of $K_{IR}3$ channels in producing an opioid-induced analgesic effect at supraspinal sites.

The present study was performed to investigate the mechanism involved in the unique *in vivo* antinociceptive effects of oxycodone at supraspinal sites. We examined whether inhibition of $K_{IR}3$ channels affected the antinociceptive effects of morphine and oxycodone by i.c.v. and intrathecal (i.t.) administration in mice. There were marked differences in the importance of $K_{IR}3$ channel function for the supraspinal antinociceptive effects between morphine and oxycodone.

Methods

Animals

Five hundred and forty C57BL/6J male mice (body wt of 18–23 g) (Charles River Laboratories Japan, Inc., Tokyo, Japan) and 42 C3H/HeN male mice (body wt of 18–23 g) (CLEA Japan, Tokyo, Japan) were used in the present study. Animals were housed in a room maintained at 23 ± 1°C under a 12 h light/dark cycle and allowed access to water and food *ad libitum*. All procedures for animal experiments were approved by the Animal Care and Use Committee of Shionogi Research Laboratories, Osaka, Japan, in agreement with the internal guidelines for animal experiments and in adherence to the ethics policy of Shionogi & Co., Ltd. (Osaka, Japan). The results of all studies involving animals are reported in accordance with the Animals in Research: Reporting In Vivo Experiments (ARRIVE) guidelines for reporting experiments involving animals (Kilkenny *et al.*, 2010; McGrath *et al.*, 2010).

Drugs

Oxycodone hydrochloride and morphine hydrochloride were obtained from Shionogi & Co., Ltd. Fentanyl citrate was obtained from Tyco Healthcare (Tyco Healthcare, Tokyo, Japan). Tertiapin-Q was purchased from Alomone Labs Ltd. (Jerusalem, Israel), and pertussis toxin (PTX) was purchased from Sigma-Aldrich (Tokyo, Japan). All drugs were dissolved in 0.9% physiological saline (Otsuka Pharmaceutical Co. Inc., Tokyo, Japan) for *in vivo* experiments and dissolved in assay buffer for *in vitro* experiments.

Tail-flick test

The antinociceptive effects of oxycodone, morphine and fentanyl were determined using the tail-flick test (Ugo-Basile, Comerio, VA, Italy) in which a heat-intensity stimulus was adjusted so that the animal flicked its tail within 4–8 s after application of the stimulus. The antinociceptive effect was expressed as a percentage of the maximal possible effect (MPE) and calculated by $(T_1 - T_0) \times 100/(T_2 - T_0)$, where T_0 and T_1 are the tail-flick latencies before and after administration of the opioid agonist, respectively, and T_2 is the cut-off time (set at 20 s) in the tests to avoid tail damage.

Drug administration i.c.v.

Drugs were administered i.c.v. as described elsewhere (Nakamura *et al.*, 2013). On the day before i.c.v. administration, a 2 mm double needle (tip: 27G, 2 mm; base: 22G, 10 mm; Natsume Seisakusyo, Tokyo, Japan) attached to a 25 μL Hamilton microsyringe was inserted into a unilateral injection site to make a hole in the skull for injection. The unilateral injection site was approximately 2 mm caudal and 2 mm lateral from the bregma, and the needle was inserted perpendicular to the skull. When drugs were administered, the injection volume was set at 2 μL for each mouse. Each solution was injected without injection cannulae.

For PTX treatments, a PTX solution (0.5 μg per mouse, i.c.v.) was administered once a day for six consecutive days.

The tail-flick test was performed on the day after the last PTX dose. For tertiapin-Q treatment, mice were pretreated with tertiapin-Q (3–30 pmol per mouse, i.c.v.) 10 min before opioid administration, and oxycodone, morphine or fentanyl was administered 10 min before measurement of the tail-flick latency or paw withdrawal response.

Drug administration i.t.

Drugs were administered i.t. as described previously (Narita *et al.*, 2008) using a 25 μL Hamilton syringe with a 30 gauge needle. The injection volume was 2 μL for each mouse. Each solution was injected without injection cannulae. For tertiapin-Q treatments, mice were pretreated with tertiapin-Q (30 pmol per mouse, i.t.) 10 min before opioid administration, and either oxycodone or morphine was administered 10 min before measurement of the tail-flick latency.

Knockdown of $K_{IR}3.1$ by siRNA

In vivo i.c.v. injection of $K_{IR}3.1$-specific siRNAs was performed in C57BL/6J male mice. The day before i.c.v. treatment, a 2 mm double needle attached to a 25 μL Hamilton microsyringe (described earlier) was inserted into a unilateral injection site to make a hole in the skull for injection. Mixtures of three different siRNAs, each possessing a unique nucleotide sequence against the mouse $K_{IR}3.1$ channel mRNA (Kcnj3: MSS 205697–205699, 500 ng per mouse; Invitrogen, Carlsbad, CA, USA), or a negative control siRNA were mixed with Invivofectamine Reagent (Invitrogen) and gently rotated for 30 min at room temperature, then diluted with 5% glucose, in accordance with the manufacturer's protocol. Injection was performed through the hole with a depth of 2 mm and repeated three times every 24 h. The tail-flick test was performed on the day following the last injection.

Western blotting analysis

The effectiveness of siRNA knockdown was confirmed by Western blotting analysis. Whole brains of the siRNA-treated mice were homogenized in lysis buffer (640 mM sucrose, 0.1 M HEPES, containing a complete mini-EDTA-free tablet; Roche, Indianapolis, IN, USA) with a high-velocity revolution homogenizer and centrifuged at 400× *g* at 4°C for 10 min. Supernatants were centrifuged at 50 000× *g* at 4°C for 30 min. The pellets were dissolved with RIPA buffer (25 mM Tris-HCl pH 7.4, 150 mM NaCl, 1% sodium deoxycholate, and 0.1% SDS), and 0.1% complete mini-EDTA-free tablet solution was added. After gentle rotation at 4°C for 30 min, samples were centrifuged again at 50 000× *g* at 4°C for 30 min, and the membrane fractions were collected from the resulting supernatants. The protein concentrations in the samples were determined using a BCA Protein Assay-Reducing Agent Compatible kit (Thermo Fisher Scientific K.K., Yokohama, Japan) according to the manufacturer's protocol. The protein samples were separated by 10% SDS-PAGE, transferred onto PVDF membranes and incubated in blocking buffer (5% skim milk in Tris-buffered saline, 0.1% Tween 20) for 60 min. The membranes were incubated with anti- $K_{IR}3.1$ channel antibody (GIRK1, H-145, sc-50410, 1:200 dilution in blocking buffer; Santa Cruz Biotechnology, Santa Cruz, CA, USA) at 4°C for 16 h, and then incubated with peroxidase-labelled anti-rabbit IgG (111-036-003, 1:5000 dilution in blocking buffer; Jackson Immuno Research Laboratories, West Grove, PA, USA) at room temperature for 1 h. Membrane-bound antibody was visualized with the ECL Plus Western Blotting Detection Reagent (GE Healthcare Life Sciences, Tokyo, Japan). Signal intensities of each band were assessed by Multi Gauge software (Fujifilm, Tokyo, Japan).

Cloning of the $K_{IR}3.1$ channel and μ-opioid receptor

The entire open reading frame (ORF) of the mouse $K_{IR}3.1$ channel and the *μ-opioid receptor 1C* were amplified by PrimeSTAR HS DNA polymerase (Takara, Shiga, Japan) from mouse brain samples by PCR under the following cycling conditions (Table 3): initial denaturation at 98°C for 2 min, followed by 30 cycles at 98°C for 10 s, annealing and extension at 68°C for 1.5 min, and a final extension at 68°C for 5 min. PCR products were subcloned into the pCR 2.1-TOPO vector (Invitrogen) using the LigaFast Rapid DNA Ligation System (Promega, Madison, WI, USA). Following ligation, plasmids were transformed into competent *Escherichia coli* DH5α cells (Toyobo, Osaka, Japan) and plated on luria broth (LB) agar containing ampicillin and isopropylthio-β-galactoside. Positive colonies were selected and incubated in LB medium containing ampicillin. Plasmid DNA was extracted using an EndoFree plasmid mega kit (Qiagen, Tokyo, Japan).

A haemagglutinin-epitope tag sequence was added between the first methionine codon and the second aspartic acid codon of the *μ-opioid receptor 1C* ORF (Table 3). This included the Kozak sequence (5′-CACC-3′) following the restriction site in the 5′ region of the first codon. Amplification was performed with PrimeSTAR HS DNA polymerase (Takara) under the following PCR cycling conditions: initial denaturation at 98°C for 2 min, followed by 30 cycles at 98°C for 10 s, annealing and extension at 68°C for 1.5 min, with a final extension at 68°C for 5 min. The entire region of *μ-opioid receptor 1C* was digested from the vector by restriction enzymes and subcloned into the pcDNA3.1(+) vector (Invitrogen). Restriction enzyme mapping and nucleotide sequencing verified insert orientation and polymerase fidelity of the constructs.

Electrophysiological recordings in Xenopus oocytes

For *in vitro* transcription, plasmids containing the entire coding sequence of the mouse *μ-opioid receptor 1C* and $K_{IR}3.1$ channel were first linearized with *EcoRI* for pcDNA3.1(+) and with *KpnI* for pCR2.1-TOPO respectively (Table 3). Capped cRNAs were synthesized from the linearized plasmids using the mMESSAGE mMACHINE T7 Ultra Kit (Ambion, Austin, TX, USA).

Mature female *Xenopus laevis* were anaesthetized by placing on ice and a small incision was made in the abdominal region. Small pieces of the ovarian lobes were dissected and gently shaken in Ca^{2+}-free modified Barth's solution (88 mM NaCl, 1.0 mM KCl, 2.4 mM $NaHCO_3$, 0.82 mM $MgSO_4$ and 7.5 mM Tris-HCl) containing 0.6 mg·mL^{-1} collagenase (Yakult, Tokyo, Japan) for 40–60 min at room temperature. Oocytes were dissociated by trituration with a fire-polished Pasteur pipette and coinjected with 12 ng of *μ-opioid receptor 1C* and 12 ng of *$K_{IR}3.1$* channel cRNAs using

an injector (Nanoject; Drummond Scientific, Broomall, PA, USA). Injected oocytes were incubated in sterile modified Barth's solution (88 mM NaCl, 1.0 mM KCl, 2.4 mM $NaHCO_3$, 0.82 mM $MgSO_4$, 7.5 mM Tris-HCl, 0.41 mM $CaCl_2$ and 0.33 mM $Ca[NO_3]_2$) at 15°C for 7–10 days.

For electrophysiological recordings, the macroscopic GIRK channel current was recorded with a two-electrode voltage clamp technique. Oocytes were voltage-clamped at –70 mV using two glass electrodes with resistances of 0.5–1.5 MΩ filled with 3 M KCl. To enable inward K^+ currents to flow through $K_{IR}3$ channels, the oocytes were infused with a high-K^+ solution (96 mM KCl, 2 mM NaCl, 1 mM $MgCl_2$ and 1.5 mM $CaCl_2$). The magnitudes of $K_{IR}3$ channel current were measured with a GeneClamp 500B amplifier (Axon Instruments, Foster City, CA, USA) and the Digidata 1332A acquisition system (Axon Instruments) and analysed with pCLAMP 10 software (Axon Instruments). All experiments were performed at room temperature.

Femur bone cancer (FBC) model

NCTC 2472 tumour cells (American Type Culture Collection, Manassas, VA, USA) were maintained in Dulbecco's Modified Eagle's Medium (Invitrogen), supplemented with 10% fetal bovine serum (Invitrogen), 100 units·mL^{-1} penicillin and 100 μg·mL^{-1} streptomycin (Invitrogen), and cultured at 37 ± 0.2°C in a humidified atmosphere of 5% CO_2. To prepare the FBC model, NCTC 2472 tumour cells were injected as described previously (Honore *et al.*, 2000; Minami *et al.*, 2009). Briefly, C3H/HeN mice were anaesthetized with 3% isoflurane, and left knee arthrotomy was performed. Tumour cells (1×10^5 cells in 5 μL of Hank's balanced salt solution) were injected directly into the medullary cavity of the distal femur, and the hole drilled in the bone was closed with resin cement (ADFA; Shofu, Kyoto, Japan). In the sham group, 5 μL of Hank's balanced salt solution was injected instead of the tumour cells in the same manner. Mice showing guarding times that changed from 0–2 s before tumour implantation to 8–16 s and displaying limb use abnormalities with a score higher than 3 (0, normal limb use; 1, slight limp; 2, obvious limp; 3, partial non-use of the limb; and 4, complete non-use of the limb) on the ipsilateral side were used for the experiments (Minami *et al.*, 2009). The effects of opioids were assessed 14 days after tumour implantation, which is the optimal time for evaluation of allodynia in this model. Allodynia-like behaviour was recognized as paw withdrawal in response to tactile stimuli using a series of von Frey monofilaments (pressure: 0.008, 0.02, 0.04, 0.07, 0.16, 0.4, 0.6 and 1 g). The up-down method of the von Frey monofilament test was used as described previously (Minami *et al.*, 2009).

Neuropathic pain model

Mice were anaesthetized with 3% isoflurane, and partial sciatic nerve injury was produced by tying a tight ligature with 8-0 silk suture (Natsume Seisakusyo, Tokyo, Japan) around approximately one-half the diameter of the sciatic nerve located on the right ipsilateral side under a light microscope (SD30; Olympus, Tokyo, Japan) as described previously (Seltzer *et al.*, 1990; Malmberg and Basbaum, 1998). In the sham group, the nerve was exposed, but no ligation was performed. The effects of opioids were assessed 7 days after sciatic nerve ligation, which is the optimal time for evaluation of allodynia in this model. Allodynia-like behaviour was evaluated using von Frey monofilaments as described previously (Minami *et al.*, 2009).

Statistical analysis

The data are shown as the means ± SEM. Statistical analyses were performed using SAS software (version 8; SAS Institute, Cary, NC, USA) and GraphPad Prism 4.0 (GraphPad Software, San Diego, CA, USA). Dose-response curves for antinociception were fitted using GraphPad Prism 4.0. The significance of differences among groups was assessed by two-way ANOVA followed by Dunnett's comparison test. Statistical analysis of differences between two groups was carried out by Student's *t*-test. In all analyses, $P < 0.05$ was taken to indicate statistical significance. The doses producing 50% of the MPE (ED_{50}) and 80% of the MPE (ED_{80}) were determined by inverse prediction based on regression analysis.

Our drug/molecular target and channel nomenclature conforms to *British Journal of Pharmacology*'s Concise Guide to PHARMACOLOGY (Alexander *et al.*, 2013).

Results

Antinociceptive effects of morphine and oxycodone by i.c.v. administration

We initially examined the antinociceptive effects of morphine and oxycodone by i.c.v. administration using the tail-flick test. Figure 1 shows that both morphine and oxycodone increased tail-flick latency in a dose-dependent manner (0.3–10 nmol per mouse) and 100% MPE was achieved at the highest dose (10 nmol per mouse) of both opioids (Figure 1A). When the time course of antinociception was examined, maximal drug effects were observed 10 min after administration of both opioids (data not shown), and this time point was used to determine ED_{50} and ED_{80} values. Figure 1B shows that the ED_{50} and ED_{80} values were similar between morphine and oxycodone, indicating that both opioid agonists possess similar antinociceptive efficacy. This was consistent with a previous report (Narita *et al.*, 2008) indicating that morphine and oxycodone have equipotent antinociceptive effects with i.c.v. administration.

The antinociceptive effect of morphine is mediated by a G protein subtype sensitive to PTX, a selective inhibitor of G_i/G_o (Hoehn *et al.*, 1988; Chang *et al.*, 1991; Shah *et al.*, 1997). However, little is known about the G protein mediating the effect of oxycodone. Therefore, we examined whether PTX-sensitive G proteins mediate the antinociceptive effect of oxycodone. In these experiments, a submaximal antinociceptive dose of 3 nmol oxycodone or morphine/mouse was administered i.c.v. Figure 1C and D show that pretreatment with PTX (0.5 μg per mouse, i.c.v.) completely blocked the antinociceptive effects of oxycodone and morphine. These results demonstrated that a PTX-sensitive G protein mediates the effects of both opioids when administered i.c.v.

Effects of tertiapin-Q on the antinociceptive effects of morphine and oxycodone

The antinociceptive effect of morphine by i.t. administration is known to be mediated by $K_{IR}3$ channels (Ikeda *et al.*, 2000;

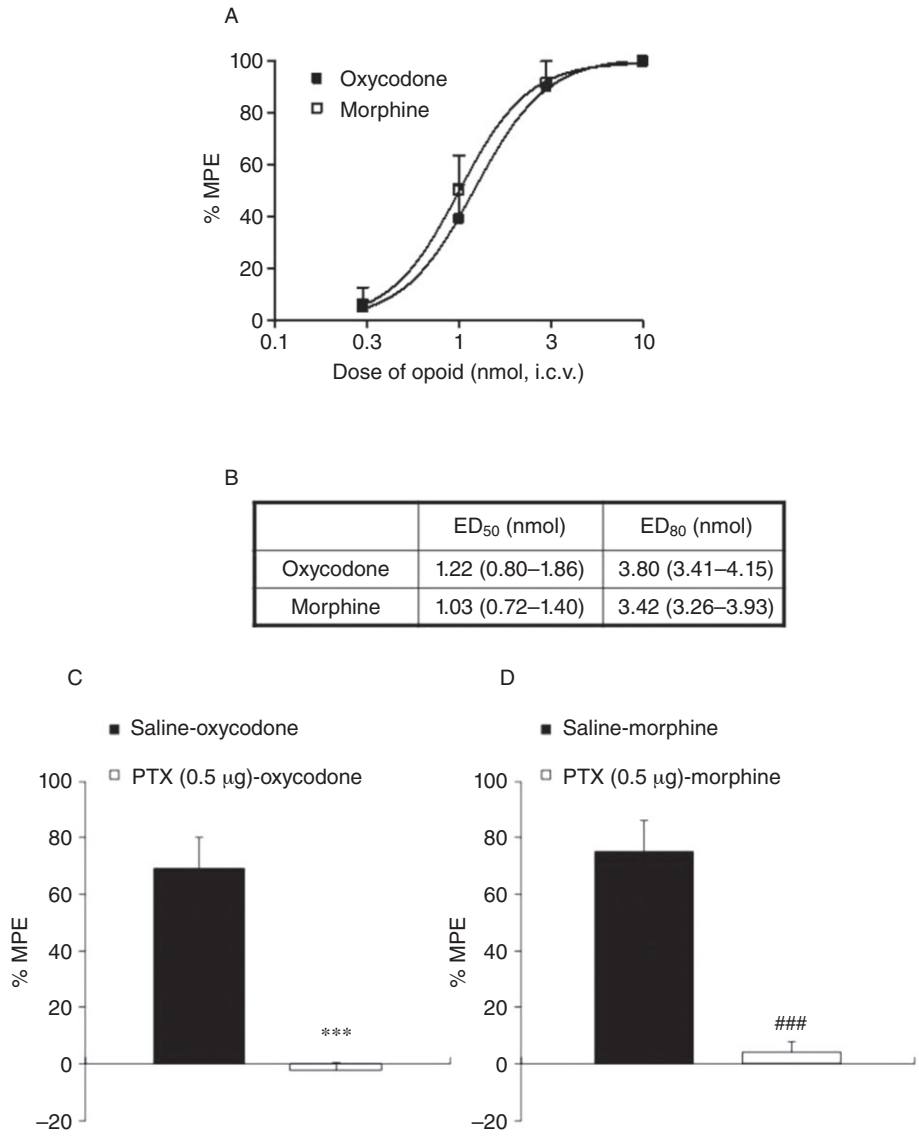

	ED_{50} (nmol)	ED_{80} (nmol)
Oxycodone	1.22 (0.80–1.86)	3.80 (3.41–4.15)
Morphine	1.03 (0.72–1.40)	3.42 (3.26–3.93)

Figure 1

Antinociceptive effects of i.c.v. morphine and oxycodone in mice tail-flick test. (A) Dose-response curves of the antinociceptive effects induced by oxycodone and morphine. Groups of mice were treated with either oxycodone or morphine (0.3–10 nmol per mouse, i.c.v.), and the antinociceptive effects were evaluated at 10 min after drug administration. The antinociceptive effects were expressed as % MPE. Data represent the mean ± SEM of 8–10 mice. (B) The ED_{50} and ED_{80} of the antinociceptive effects of oxycodone and morphine. Effects of PTX on (C) oxycodone- and (D) morphine-induced antinociception in the mice tail-flick test. Mice were pretreated with PTX (0.5 μg per mouse, i.c.v.) once a day for 6 consecutive days. The tail-flick latency was measured on the next day after the last PTX administration. Either oxycodone (3 nmol per mouse, i.c.v.) or morphine (3 nmol per mouse, i.c.v.) was administered 10 min before evaluation of the tail-flick latency. The antinociceptive effects are expressed as %MPE. Data represent the mean ± SEM of 6–8 mice. ***$P < 0.001$ versus saline-oxycodone group, ###$P < 0.001$ versus saline-morphine group (two-way ANOVA, Student's *t*-test).

Marker *et al.*, 2002; 2004; Mitrovic *et al.*, 2003), but the role of $K_{IR}3$ channels in the antinociceptive effects at supraspinal sites is largely unknown. Therefore, we examined whether $K_{IR}3$ channels are involved in the antinociceptive effects of morphine and oxycodone following i.c.v. administration. When mice were treated with the $K_{IR}3$ channel blocker tertiapin-Q, the antinociceptive effect of oxycodone (3 nmol per mouse, i.c.v.) was markedly attenuated in a dose-dependent manner (Figure 2). In contrast, the antinociceptive effect of morphine (3 nmol per mouse, i.c.v.) was unaffected by tertiapin-Q treatment, and the effect of morphine remained at 92.7% MPE when the highest dose (30 pmol per mouse) of tertiapin-Q was administered (Figure 2). These results indicate that the underlying antinociceptive mechanisms differ between morphine and oxycodone at supraspinal sites, and that a tertiapin-Q-sensitive mechanism mediates the effect of oxycodone in an agonist-dependent manner.

We further investigated the importance of $K_{IR}3$ channel activation in the antinociceptive effects of morphine and oxycodone by comparing dose-response curves of the opioid agonists in the presence or absence of tertiapin-Q. Both i.c.v. administration of oxycodone (0.3–100 nmol per mouse) and morphine (0.3–10 nmol per mouse) produced antinociceptive effects in a dose-dependent manner (Figure 3A, B), while tertiapin-Q treatment (30 pmol per mouse, i.c.v.) in the oxycodone treatment group produced a greater rightward shift in the dose-response curve compared with that in the morphine treatment group (Figure 3A, B). Table 1 shows the relative potency determined as the shift ratio (T/V) of the ED_{50} values between the tertiapin-Q-treated group (T) and the vehicle-treated group (V) for each opioid. While oxycodone produced a large difference in the ED_{50} values between the two groups with a shift ratio of 7.09, morphine exhibited only a small difference with a shift ratio of 1.43, confirming differences in the tertiapin-Q-sensitive mechanism between morphine and oxycodone at supraspinal sites (Table 1).

Since, we found for the first time that the importance of the tertiapin-Q-sensitive mechanism differed between oxycodone and morphine, we then examined the role of the tertiapin-Q-sensitive mechanism in the antinociceptive effect of fentanyl, another clinically used potent μ-opioid receptor agonist. As the maximal antinociceptive effect of fentanyl was observed 10 min after i.c.v. administration (data not shown), we evaluated the effect of fentanyl at this time point.

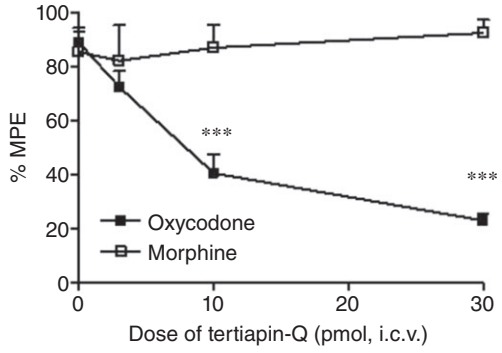

Figure 2

Effects of tertiapin-Q on oxycodone- and morphine-induced antinociception after i.c.v. administration in mice tail-flick test. Groups of mice were treated with tertiapin-Q (3–30 mol per mouse, i.c.v.) 10 min before the opioids, either oxycodone (3 nmol per mouse, i.c.v.) or morphine (3 nmol per mouse, i.c.v.) was administered 10 min before evaluation of the tail-flick latency. The antinociceptive effects are expressed as %MPE. Data represent the mean ± SEM of 6–10 mice. ***P < 0.001 versus morphine group (two-way ANOVA, Dunnett's multiple comparison test).

Table 1

The ED_{50} of the antinociceptive effects of i.c.v. oxycodone and morphine

ED_{50} (nmol)	Vehicle	Tertiapin-Q	Shift ratio (T/V)
Oxycodone	1.29 (0.82–2.03)	9.15 (6.12–13.68)	7.09
Morphine	1.57 (1.05–2.36)	2.24 (1.59–3.18)	1.43

The ED_{50} values were determined by linear regression using data from at least four doses in each opioid. Values in parentheses indicate the 95 % confidence range. The shift ratio (T/V) represents relative potency of the ED_{50} values between vehicle group (V) and tertiapin-Q group (T). The ratio (O/M) represents relative efficacy of oxycodone over that of morphine.

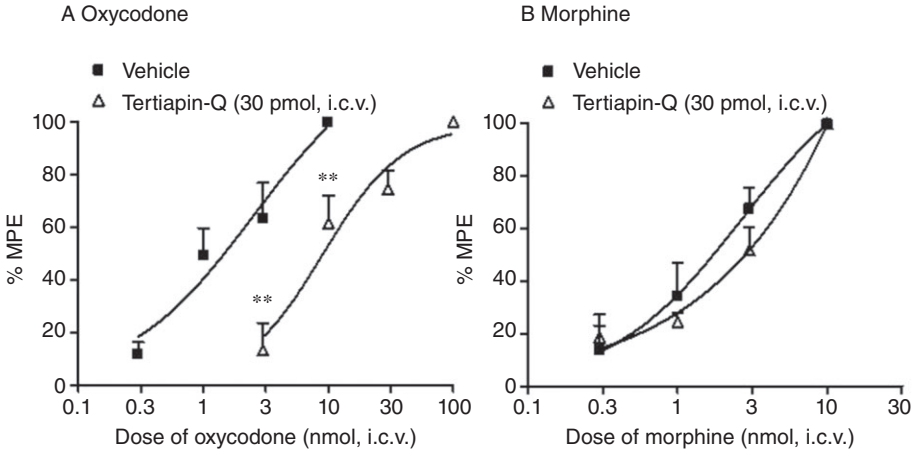

Figure 3

Dose-dependent antinociceptive effects induced by i.c.v. administration of oxycodone and morphine in the presence of tertiapin-Q in mice tail-flick test. Groups of mice were pretreated with tertiapin-Q (30 pmol per mouse) 10 min before the opioids. The administration route of tertiapin-Q was the same as that of respective opioid administration in each experimental group. Oxycodone (A: 0.3–100 nmol per mouse, i.c.v.) or morphine (B: 0.3–10 nmol per mouse, i.c.v.) was administered 10 min before evaluation of the tail-flick latency. The antinociceptive effects are expressed as %MPE. Data represent the mean ± SEM of eight mice. **P < 0.01 versus vehicle-oxycodone group (two-way ANOVA, Dunnett's multiple comparison test).

As shown in Figure 4, i.c.v. administration of fentanyl (0.1–1.7 nmol per mouse) produced a dose-dependent antinociceptive effect. When mice were treated with fentanyl in the presence of tertiapin-Q (30 pmol per mouse, i.c.v.), the effect of fentanyl was attenuated. However, the attenuation was much smaller than that observed with oxycodone, and the shift ratio (T/V) of ED_{50} value was 1.46 (ED_{50} = 0.23 nmol per mouse in the vehicle group, 0.33 nmol per mouse in the tertiapin-Q group), which was similar to that of morphine.

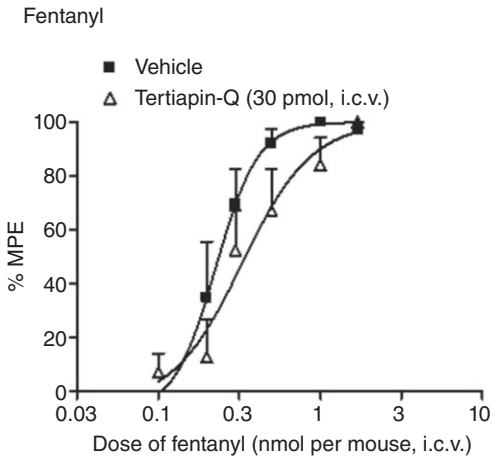

Figure 4

Dose-dependent antinociceptive effect induced by i.c.v. administration of fentanyl in the presence of tertiapin-Q in mice tail-flick test. Groups of mice were pretreated with tertiapin-Q (30 pmol per mouse) 10 min before fentanyl. Fentanyl (0.1–1.7 nmol per mouse, i.c.v.) was administered 10 min before evaluation of the tail-flick latency. The antinociceptive effect is expressed as %MPE. Data represent the mean ± SEM of 5–10 mice.

Thus, the tertiapin-Q-sensitive mechanism plays a primary role in the antinociceptive effect of oxycodone, but not morphine and fentanyl, at supraspinal sites.

We next examined the effect of tertiapin-Q on the antinociceptive effect of morphine and oxycodone induced by i.t. administration. As the time course experiment showed maximal drug effects 10 min after i.t. administration for both opioids (data not shown), the drug effects were determined at this time point. The results indicated that both oxycodone (1–100 nmol per mouse, i.t.) and morphine (0.1–10 nmol pe mouse, i.t.) exhibited dose-dependent antinociceptive effects (Figure 5A, B), and tertiapin-Q treatment (30 pmol per mouse, i.t.) significantly and similarly attenuated the effects of the respective opioids (Figure 5A, B). Table 2 shows the relative potency determined as the shift ratio of the ED_{50} values (T/V) between the tertiapin-Q-treated group (T) and the vehicle-treated group (V) for each opioid; the effects of

Table 2

The ED_{50} of the antinociceptive effects of i.t. oxycodone and morphine

ED_{50} (nmol)	Vehicle	Tertiapin-Q	Shift ratio (T/V)
Oxycodone	3.51 (2.04–6.05)	15.58 (9.03–26.9)	4.44
Morphine	0.28 (0.17–0.48)	1.48 (0.73–3.01)	5.29

The ED_{50} values were determined by linear regression using data from at least four doses for each opioid. Values in parentheses indicate the 95% confidence range. The shift ratio (T/V) shows relative potency of the ED_{50} values between vehicle group (V) and tertiapin-Q group (T). The ratio (O/M) represents relative efficacy of oxycodone over that of morphine.

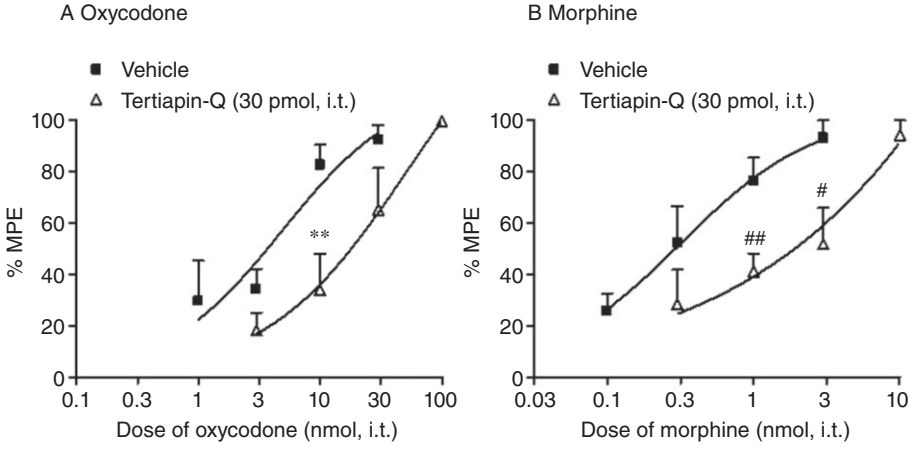

Figure 5

Dose-dependent antinociceptive effects induced by i.t. administration of oxycodone and morphine in the presence of tertiapin-Q in mice tail-flick test. Groups of mice were pretreated with tertiapin-Q (30 pmol per mouse) 10 min before the opioids. The administration route of tertiapin-Q was the same as that of respective opioid administration in each experimental group. Oxycodone (A: 1–100 nmol per mouse, i.t.) or morphine (B: 0.1–10 nmol per mouse, i.t.) was administered 10 min before evaluation of the tail-flick latency. The antinociceptive effects are expressed as %MPE. Data represent the mean ± S.E.M. of eight mice. $^{**}P < 0.01$ versus vehicle-oxycodone group, $\#P < 0.05$ or $\#\#P < 0.01$ versus vehicle-morphine group (two-way ANOVA, Dunnett's multiple comparison test).

Table 3

Primer sequences used for the cloning of mouse *μ-opioid receptor 1C* and $K_{IR}3.1$ channel

The following sequences were used for *μ-opioid receptor 1C* cloning	
First PCR,	Forward 5′-CGAGTCCGCAGCAAGCATTCAGAACCATGGAC-3′ Reverse 5′-TCACCTGCCAAGCTGGCCTTCC-3′
Nested PCR,	Forward 5′-ATGGACAGCAGCGCCGGCCC-3′ Reverse 5′-TCACCTGCCAAGCTGGCCTTCCCCGGATTCCTG-3′
For the HA tag insertion in *μ-opioid receptor 1C*	
First PCR,	Forward 5′-CATACGATGTTCCAGATTACGCT**GAC**AGCAGCGCCGGCCCAG-3′ Reverse 5′-TCACCTGCCAAGCTGGCCTTCCCCGGATTCCTG-3′
Second PCR	Forward 5′-TTAAAA*AAGCTT*cacc**ATG**TACCCATACGATGTTCCAGATTACGCTG-3′ Reverse 5′-TTAAAA*GAATTC*ACCTGCCAAGCTGGCCTTC-3′
The following sequences were used for $K_{IR}3.1$ cloning	
	Forward 5′-GTATTATGTCTGCACTCCGAAGGA-3′ Reverse 5′-TTTTGCTATGTGAAACGGTCAGAGTT-3′

As for *μ-opioid receptor 1C*, the entire ORF was amplified by the primer sets of first PCR and nested PCRs. After being ligated to pCR 2.1 TOPO vector, HA tag sequence was inserted between the first and the second codon of the *μ-opioid receptor 1C*. In this case, for the first PCR, 3′ sequence of the HA tag (underline) was inserted before the second codon (bold). For the second PCR, restriction enzyme (*Hind III*) (italic) and kozac (lower case) sequences were added before the first codon (bold). In addition, the 5′ sequence of the HA tag (underline) was added after the first codon. *EcoR* I (italic) was added at the 3′ end of the ORF.
HA, haemagglutinin.

both oxycodone and morphine were attenuated to a similar extent (shift ratio of oxycodone = 4.44, shift ratio of morphine = 5.29). This result indicates that a tertiapin-Q-sensitive mechanism plays an important role in for both the oxycodone- and morphine-induced antinociceptive effects at spinal sites.

Role of $K_{IR}3.1$ channels in the antinociceptive effect of oxycodone administered i.c.v.

Although tertiapin-Q is known to be a specific blocker of $K_{IR}3$ channels, it is important to confirm whether the observed effect of tertiapin-Q is due to inhibition of $K_{IR}3$ channels using a different approach. It has been reported that tertiapin-Q strongly inhibits $K_{IR}3.1$ and $K_{IR}3.4$ channel activities (Jin and Lu, 1998), and the level of $K_{IR}3.4$ channel expression is lower than those of other $K_{IR}3$ channels ($K_{IR}3.1$–3.3) in the brain. Therefore, we focussed on $K_{IR}3.1$ channels and employed an *in vivo* knockdown approach using siRNA to inhibit $K_{IR}3.1$ channel activity.

We first evaluated $K_{IR}3.1$ channel knockdown at supraspinal sites by i.c.v. administration of $K_{IR}3.1$ channel siRNA. Western blotting analysis showed that $K_{IR}3.1$ channel protein level was significantly decreased in the brains of mice treated with the $K_{IR}3.1$ channel siRNA (Figure 6A). Using this knockdown protocol, we next examined whether the antinociceptive effects of oxycodone and morphine were attenuated in the tail-flick test. The results confirmed that knockdown of $K_{IR}3.1$ channel expression had no significant effect on the basal tail-flick latency (control siRNA: 6.05 ± 0.66 s, $K_{IR}3.1$ siRNA: 4.91 ± 0.32 s), and no obvious behavioural change was observed under our experimental conditions. When $K_{IR}3.1$ channels were inhibited by siRNA treatment, the antinociceptive effect of oxycodone (3 nmol per mouse, i.c.v.) was significantly attenuated, whereas the effect of morphine (3 nmol per mouse, i.c.v.) was virtually unaffected (Figure 6B). These results were consistent with the observations from the earlier experiments using tertiapin-Q, and we concluded that the antinociceptive role of $K_{IR}3.1$ channels at supraspinal sites is different between oxycodone and morphine.

Increase in K^+ channel current by opioid agonists and inhibition by tertiapin-Q in Xenopus oocytes coexpressing both μ-opioid receptor 1C and $K_{IR}3.1$ channels

We next investigated whether tertiapin-Q had the expected inhibitory effect on opioid-induced $K_{IR}3.1$ channel activation using *Xenopus* oocyte-mediated gene expression. In oocytes coinjected with mouse *μ-opioid receptor 1C* and *$K_{IR}3.1$* channel cRNAs, oxycodone (0.1–100 μM) and morphine (0.01–10 μM) evoked inward currents in a concentration-dependent manner. The EC_{50} values of oxycodone and morphine were 3.5 and 0.18 μM, and the maximum currents of oxycodone and morphine were observed at 100 and 10 μM respectively (data not shown). When tertiapin-Q (100 nM) was applied simultaneously with either oxycodone (100 μM) or morphine (10 μM), the inward currents evoked by the respective opioids were significantly inhibited in a similar manner (Figure 7). Although tertiapin-Q (100 nM) alone changed the baseline current, this change was predicted under the experimental conditions due to the presence of high levels of potassium, and this has been reported to not affect interpretation of the opioid effect (Yow *et al.*, 2011). These results indicate that tertiapin-Q produced the expected inhibitory effect on opioid-induced $K_{IR}3.1$ channel activity.

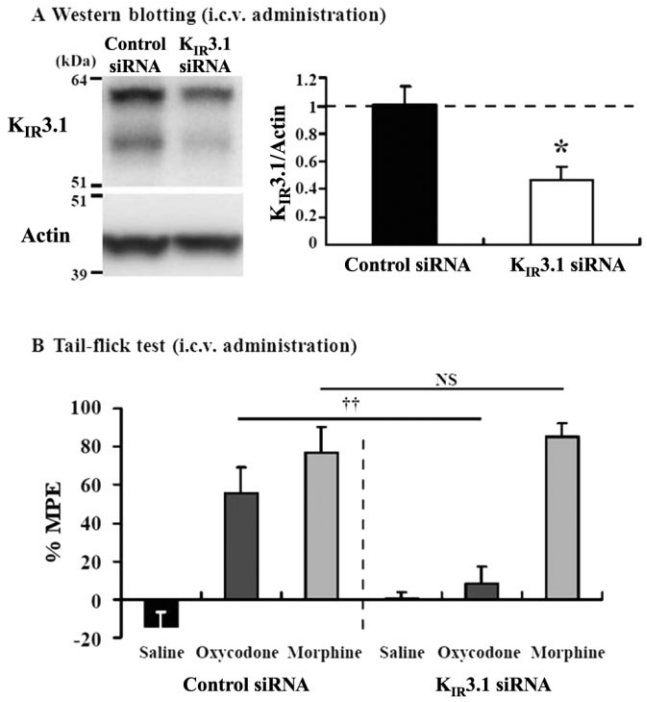

Figure 6

Effects of $K_{IR}3.1$ channel siRNA on antinociceptive effects of i.c.v. morphine and oxycodone in mice tail-flick test. (A) The Western blot analysis showed that the $K_{IR}3.1$ channel protein level was decreased in mice whole brain without cerebellum after the $K_{IR}3.1$ channel siRNA treatment. The $K_{IR}3.1$ channel siRNA was administered repeatedly once a day for 3 consecutive days, and the whole brain membrane fraction was prepared on the next day after the last administration. The brain samples were analysed using SDS-PAGE. The gel image (A) shows a representative result, and similar results were obtained in two independent experiments. Quantification of $K_{IR}3.1$ channel protein level was calculated by two bands. The columns represent the relative protein levels (the mean protein level in the control siRNA-treated group was defined as 1.0) in the groups treated with control siRNA and $K_{IR}3.1$ channel siRNA respectively. The mean ± SEM of three to four independent experiments are shown. *P < 0.05 versus control siRNA group (two-way ANOVA, Student's t-test). (B) Antinociceptive effects of oxycodone and morphine in $K_{IR}3.1$ channel knockdown mice examined by tail-flick test. Groups of mice were pretreated with $K_{IR}3.1$ channel siRNA (500 ng per mouse, i.c.v., once a day for three consecutive days) before opioid administration, and either oxycodone or morphine (3 nmol per mouse, i.c.v.) was administered 10 min before evaluation of the tail-flick latency. The antinociceptive effects are expressed as %MPE. Data represent the mean + SEM of 8–10 mice. ††P < 0.01, two-way ANOVA; *post hoc* Dunnett's test.

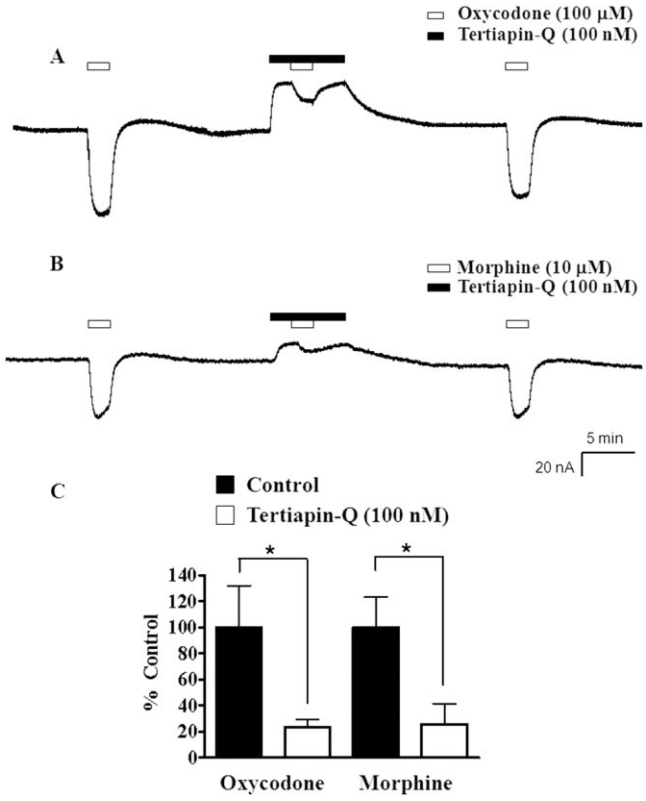

Figure 7

Effects of tertiapin-Q on oxycodone- and morphine-induced $K_{IR}3.1$ channel activation in *Xenopus* oocytes. The data presented are typical recordings of K^+ channel current by (A) oxycodone and (B) morphine. Representative current responses to oxycodone (100 μM) and morphine (10 μM) in the presence of tertiapin-Q (100 nM) in an oocyte co-injected with *μ-opioid receptor 1C* and *$K_{IR}3.1$* channel cRNAs. (C) Effects of tertiapine-Q (100 nM) on currents evoked by oxycodone (100 μM) or morphine (10 μM). The columns represent the relative K^+ channel activities (the mean activity in the each control of oxycodone or morphine was defined as 100%) in the control and tertiapin-Q-treated groups. Values are means ± SEM of four independent samples. *P < 0.05 versus. control (Student's t-test).

Effects of tertiapin-Q on the antinociceptive effects of oxycodone in chronic pain models

The earlier experiments, using the tail-flick test in normal mice, indicated a significant role for supraspinal $K_{IR}3$ channels in mediating the antinociceptive effects of oxycodone. However, it is also important to investigate the role of $K_{IR}3.1$ channels in opioid-induced analgesia in chronic pain models. Therefore, we investigated the effects of tertiapin-Q on the antinociceptive effects of morphine and oxycodone in FBC and neuropathic pain models. We first determined optimal doses of systemically administered morphine and oxycodone in these two pain models and found that morphine at 30 mg·kg^{-1} and oxycodone at 5.6 mg·kg^{-1} exhibited similar submaximal antinociceptive effects in both models. These doses were subsequently used to evaluate the effects of tertiapin-Q. Administration of oxycodone (5.6 mg·kg^{-1}, s.c.) significantly restored the decreased paw withdrawal threshold in the FBC model (Figure 8A), and pretreatment with tertiapin-Q (30 pmol per mouse, i.c.v.) significantly attenuated this antinociceptive effect of oxycodone. In contrast, the same tertiapin-Q treatment had no effect on the antinociceptive effect of morphine (30 mg·kg^{-1}, s.c.) in the FBC model. A similar result was observed in the neuropathic pain model, where the antinociceptive effect of oxycodone (5.6 mg·kg^{-1}, s.c.) was markedly attenuated by treatment with tertiapin-Q (30 pmol per mouse, i.c.v.), whereas that induced by morphine was little affected by tertiapin-Q (30 pmol per mouse,

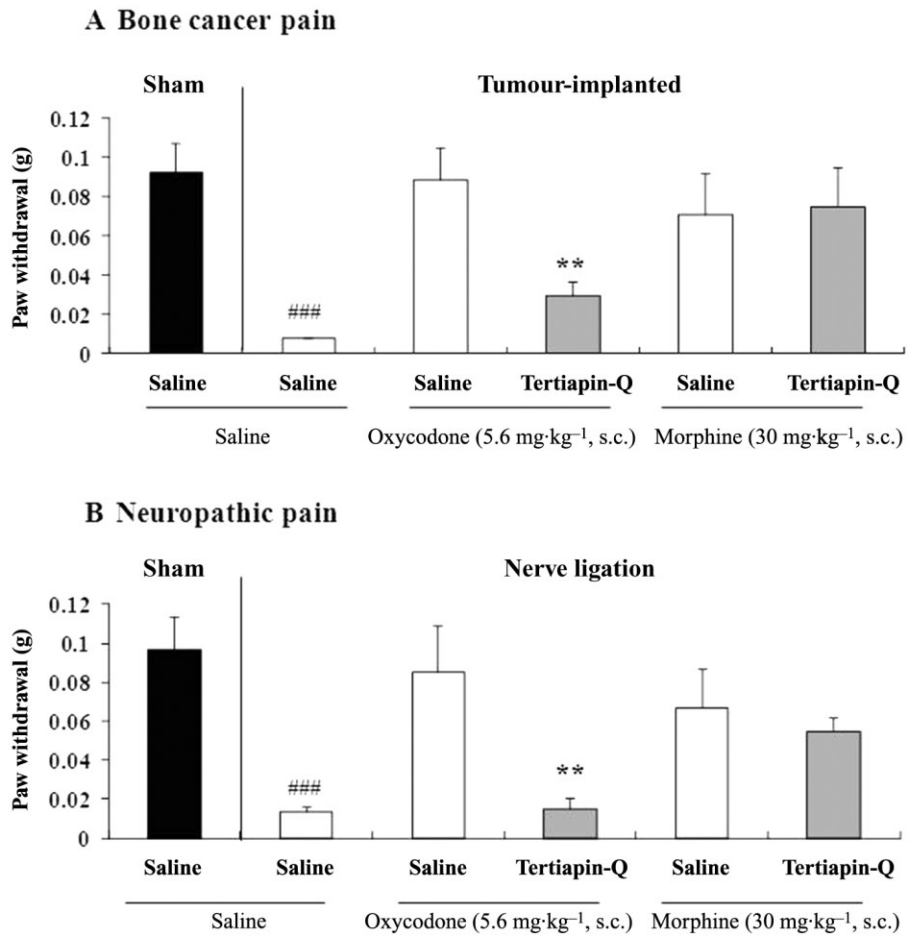

Figure 8

Effects of tertiapin-Q on oxycodone- and morphine-induced antinociceptive effects in the (A) FBC and (B) neuropathic pain models. Groups of mice were treated with tertiapin-Q (30 pmol per mouse, i.c.v.) 10 min before the opioids, and either oxycodone (5.6 mg·kg^{-1}, s.c.) or morphine (30 mg·kg^{-1}, s.c.) was systemically administered 15 or 30 min before evaluation of the paw withdrawal by von Frey test. The *y*-axes show thresholds of paw withdrawal response, and data represent the mean ± SEM of 6–8 mice in each group. The columns show (A) tumour-implanted group or (B) nerve ligation group. $^{**}P < 0.01$ versus tumour-implanted or ligation-saline-oxycodone group, $^{###}P < 0.001$ versus sham-saline-saline group (two-way ANOVA, Dunnett's multiple comparison test).

i.c.v.) (Figure 8B). These results indicate that, in addition to the differential antinociceptive effects in normal animals, antinociceptive effects in the chronic pain models are mediated by different signalling mechanisms at supraspinal sites and that $K_{IR}3.1$ channels in the brain play a primary role in the effects of oxycodone, but not in those of morphine.

Discussion

In the present study, we demonstrated that inhibition of $K_{IR}3.1$ channels significantly attenuated the antinociceptive effects of i.c.v. oxycodone administration, whereas the antinociceptive effects of morphine were unaffected by either pharmacological or biochemical $K_{IR}3.1$ channel inhibition. These results show that roles of $K_{IR}3.1$ channels in the mechanisms of the antinociceptive effects differ between morphine and oxycodone at the supraspinal sites, and that activation of $K_{IR}3.1$ channels is required for the intrinsic antinociceptive effect of oxycodone at supraspinal sites, but not for that of morphine.

The differential role of $K_{IR}3.1$ channels in the antinociceptive effects of morphine and oxycodone was observed not only with nociceptive pain in normal mice but also during allodynia in the chronic pain models. We chose the FBC and neuropathic pain models as chronic pain models as μ-opioid receptor agonists have frequently been prescribed to control bone cancer pain and neuropathic pain in clinical settings (Mercadante and Arcuri, 1998; Portenoy *et al.*, 1999). The FBC model (Honore *et al.*, 2000; Minami *et al.*, 2009) mimics several clinical features of human bone cancer pain (Komiya *et al.*, 1999; Pandit-Taskar *et al.*, 2004), and the neuropathic pain model produces abnormal pain characterized by hyperalgesia and allodynia. Using these two pain models, we found that the antinociceptive effect of oxycodone, but not morphine, was strongly attenuated in the presence of tertiapin-Q,

indicating the importance of functional $K_{IR}3.1$ channels in this opioid-dependent antinociceptive effect. One alternative interpretation of the present data is that systemically administered morphine was not distributed at sufficiently high concentrations in the brain to produce an antinociceptive effect at the supraspinal level in these two pain models, and hence, the effect of morphine was unaffected by the i.c.v. administration of tertiapin-Q. However, our preliminary data showed that when an antinociceptive dose of morphine was administered systemically in these two models, the levels of morphine were similar in the spinal cord and several brain regions (data not shown). It is unlikely, therefore, that the level of morphine in the brain was too low to produce the antinociceptive effect after systemic administration. Thus, the differential antinociceptive role of $K_{IR}3.1$ channels at supraspinal sites was not only specific to nociceptive pain in normal animals but was also applicable to chronic pain conditions.

In contrast to the effects induced by i.c.v. administration, the antinociceptive effects of i.t. administration of oxycodone and morphine were similarly inhibited by tertiapin-Q. These observations indicate that $K_{IR}3.1$ channels play a comparable role in the antinociceptive effects of both opioids at spinal sites. It has been reported that $K_{IR}3.1/2$ channel complexes at the spinal cord modulate thermal nociception and mediate the analgesic effect of morphine (Marker *et al.*, 2002; 2004). Our data were consistent with these results in terms of the importance of $K_{IR}3.1$ channels for the morphine-induced antinociceptive effect at spinal sites.

Oxycodone and morphine are μ-opioid receptor agonists (Narita *et al.*, 2008; Nakamura *et al.*, 2013). We showed here that both opioids exhibited their antinociceptive effects via a PTX-sensitive G protein, but the importance of $K_{IR}3.1$ channels was different between the antinociceptive effects of oxycodone and morphine at supraspinal sites. Currently, little is known about an underlying mechanism for this opioid-dependent role of $K_{IR}3.1$ channels in the antinociceptive effects. We also showed that $K_{IR}3.1$ channels were differently involved in the antinociceptive effect of morphine between the spinal cord and the brain. This is consistent with findings from previous studies observed in $K_{IR}3.1$channel-knockout mice. In these $K_{IR}3.1$ channel-knockout mice the morphine-induced K^+ channel current in locus ceruleus slices was abolished, but the antinociceptive effect of morphine at supraspinal sites was shown to be preserved, whereas the morphine withdrawal syndrome was strongly attenuated (Cruz *et al.*, 2008), indicating that supraspinal $K_{IR}3.1$ channel activation does not play a primary role in the antinociceptive effect of morphine. In contrast, morphine-induced antinociception at spinal sites was attenuated in other $K_{IR}3$ channel knockout mice (Marker *et al.*, 2002; 2004). Taken together, these results suggest that morphine activates $K_{IR}3.1$ channels at both spinal sites and the brain, but that the importance of $K_{IR}3.1$ channel function in its nociceptive effects differs and is dependent on the site of action of morphine. In the present study, we demonstrated such region-dependent difference in the roles of $K_{IR}3$ channels for the morphine antinociception in comparable experimental settings between spinal sites and the brain. This tissue-specific signalling mechanism is of great interest in the elucidation of the physiological effects of opioids.

Among the various metabolites of oxycodone, oxymorphone is produced by CYP2D6 and is known to possess high affinity and potent efficacy as an agonist at μ-opioid receptors (Lemberg *et al.*, 2006; Peckham and Traynor, 2006). While the amount of oxymorphone produced by i.c.v. and i.t. administrations of oxycodone appears to be little in our experimental scheme, systemic administration of oxycodone, such as s.c., might produce a significant amount of oxymorphone. This suggests that the observed antinociceptive effects induced by s.c. administration of oxycodone in the pain models were the sum of the effects of both oxycodone and oxymorphone. It appears that there are species differences in the extent that oxymorphone contributes to the effects of oxycodone after systemic administration. Although the contribution of oxymorphone to oxycodone-induced analgesia is minimal in humans (Klimas *et al.*, 2013), oxymorphone does contribute to the antinociceptive effects of oxycodone in rats (Lemberg *et al.*, 2006). As little is known about how much oxymorphone is produced in mice, we cannot completely rule out the possibility that oxymorphone induced some of the antinociceptive effects attributed to oxycodone in the present study, especially after s.c. administration.

In conclusion, this study demonstrated that $K_{IR}3.1$ channels play a primary role in the antinociceptive effect of oxycodone, but not those of morphine at supraspinal sites. To our knowledge, this is the first study demonstrating differential roles of $K_{IR}3.1$ channels in the antinociceptive effects of oxycodone and morphine. The data suggest that these differences in $K_{IR}3.1$ channel function at supraspinal sites are responsible for the paradoxically potent antinociceptive effect of oxycodone compared with morphine. In addition, we also demonstrated differential roles of $K_{IR}3.1$ channels in mediating the antinociceptive effects of morphine at the spinal cord and in the brain. Further studies are required to determine how this opioid-dependent at supraspinal sites, and region-specific function of $K_{IR}3$ channels were originated.

Conflict of interest

None of the authors have any conflicts of interest to disclose relating to this submission. A N, M F, H O, Y H, T K, K O, Y M, A N, G S, A K and M H are employees of Shionogi Co., Ltd, the manufacturer of oxycodone and morphine.

References

Alexander SPH *et al.* (2013). The Concise Guide to PHARMACOLOGY 2013/14: Overview. Br J Pharmacol 170: 1449–1867.

Bercovitch M, Adunsky A (2006). High dose controlled-release oxycodone in hospice care. J Pain Palliat Care Pharmacother 20: 33–39.

Bostrom E, Simonsson US, Hammarlund-Udenase M (2006). In vivo blood-brain barrier transport of oxycodone in the rat: indications for active influx and implications for pharmacokinetics/pharmacodynamics. Drug Metab Dispos 34: 1624–1631.

Bostrom E, Hammarlund-Udenase M, Simonsson US (2008). Blood-brain barrier transport helps to explain discrepancies in in vivo potency between oxycodone and morphine. Anesthesiology 108: 495–505.

Chang SC, Lutfy K, Sierra V, Yoburn BC (1991). Dissociation of opioid receptor upregulation and functional supersensitivity. Pharmacol Biochem Behav 38: 853–859.

Cruz HG, Berton F, Sollini M, Blanchet C, Pravetoni M, Wickman K *et al*. (2008). Absence and rescue of morphine withdrawal in GIRK/Kir3 knock-out mice. J Neurosci 9: 4069–4077.

Heiskanen T, Kalso E (1997). Controlled-release oxycodone and morphine in cancer related pain. Pain 73: 37–45.

Hoehn K, Reid A, Sawynok J (1988). Pertussis toxin inhibits antinociception produced by intrathecal injection of morphine, noradrenaline and baclofen. Eur J Pharmacol 27: 65–72.

Honore P, Lugar NM, Sabino MAC, Schwei MJ, Rogers SD, Mash DB *et al*. (2000). Osteroprotegerin blocks bone cancer-induced skeletal destruction, skeletal pain and pain-induced neurochemical reorganization of the spinal cord. Nat Med 6: 521–528.

Ikeda K, Kobayashi T, Kumanishi T, Niki H, Yano R (2000). Involvement of G-protein-activated rectifying K (GIRK) channels in opioid-induced analgesia. Neurosci Res 38: 113–116.

Jin W, Lu Z (1998). A novel high-affinity inhibitor for inward-rectifier K+ channels. Biochemistry 37: 13291–13299.

Kilkenny C, Browne W, Cuthill IC, Emerson M, Altman DG (2010). Animal research: reporting *in vivo* experiments: the ARRIVE guidelines. Br J Pharmacol 160: 1577–1579.

Klimas R, Witticke D, El Fallsh S, Mikus G (2013). Contribution of oxycodone and its metabolites to the overall analgesic effect after oxycodone administration. Expert Opin Drug Metab Toxicol 9: 517–528.

Komiya S, Zenmyo M, Inoue A (1999). Bone tumors in the pelvis presenting growth during pregnancy. Arch Orthop Trauma Surg 119: 22–29.

Koyyalagunta D, Bruera E, Solanki DR, Nouri KH, Burton AW, Toro MP *et al*. (2012). A systematic review of randomized trials on the effectiveness of opioids for cancer pain. Pain Physician 15: ES39–ES58.

Lemberg KK, Kontinen VK, Siiskonen AO, Viljakka KM, Yli-Kauhaluoma JT, Korpi ER *et al*. (2006). Antinociception by spinal and systemic oxycodone: why does the route make a difference? In vitro and in vivo studies in rats. Anesthesiology 105: 801–812.

McGrath J, Drummond G, McLachlan E, Kilkenny C, Wainwright C (2010). Guidelines for reporting experiments involving animals: the ARRIVE guidelines. Br J Pharmacol 160: 1573–1576.

Malmberg AB, Basbaum AI (1998). Partial sciatic nerve injury in the mouse as a model of neuropathic pain: behavioral and neuroanatomical correlates. Pain 76: 215–222.

Marker CL, Cintora SC, Roman MI, Stoffel M, Wickman K (2002). Hyperalgesia and blunted morphine analgesia in G protein-gated potassium channel subunit knockout mice. Neuroreport 20: 2509–2513.

Marker CL, Stoffel M, Wickman K (2004). Spinal G-protein-gated K+ channels formed by GIRK1 and GIRK2 subunits modulate thermal nociception and contribute to morphine analgesia. J Neurosci 17: 2806–2812.

Mercadante S, Arcuri E (1998). Breakthrough pain in cancer patients: pathophysiology and treatment. Cancer Treat Rev 24: 425–432.

Minami K, Hasegawa M, Ito H, Nakamura A, Tomii T, Matsumoto M *et al*. (2009). Morphine, oxycodone, and fentanyl exhibit different analgesic profiles in mouse pain models. J Pharmacol Sci 111: 60–72.

Mitrovic I, Margeta-Mitrovic M, Bader S, Stoffel M, Jan LY, Basbaum AI (2003). Contribution of GIRK2-mediated postsynaptic signaling to opiate and alpha2-adrenergic analgesia and analgesic sex differences. Proc Nalt Acad Sci USA 100: 271–276.

Moulin DE, Iezzi A, Ameireh R, Sharpe WKJ, Boyd D, Merskey H (1996). Randomised trial of oral morphine for chronic non-cancer pain. Lancet 347: 143–147.

Nakamura A, Hasegawa M, Minami K, Kanbara T, Tomii T, Nishiyori A *et al*. (2013). Differential activation of the μ-opioid receptor by oxycodone and morphine in pain-related brain regions in a bone cancer pain model. Br J Pharmacol 168: 375–388.

Narita M, Nakamura A, Ozaki M, Imai S, Miyoshi K, Suzuki M *et al*. (2008). Comparative pharmacological profiles of morphine and oxycodone under a neuropathic pain-like state in mice: evidence for less sensitivity to morphine. Neuropsychopharmacology 33: 1097–1112.

Pandit-Taskar N, Batraki M, Divgi CR (2004). Radiopharmaceutical therapy for palliation of bone pain from osseous metastases. J Nucl Med 45: 1358–1365.

Peckham EM, Traynor JR (2006). Comparison of the antinociceptive response to morphine and morphine-like compounds in male and female Sprague-Dawley rats. J Pharmacol Exp Ther 316: 1195–1201.

Portenoy RK, Payne D, Jacobsen P (1999). Breakthrough pain: characteristics and impact in patients with cancer pain. Pain 81: 129–134.

Seltzer D, Dubner R, Shir Y (1990). A novel behavioral model of neuropathic pain disorders produced in rats by partial sciatic nerve injury. Pain 43: 205–218.

Shah S, Breivogel C, Selly D, Munirathinam G, Childers S, Yoburn BC (1997). Time-dependent effects of in vivo pertussis toxin on morphine analgesia and G-proteins in mice. Pharmacol Biochem Behav 56: 465–469.

Silvestri B, Bandieri E, Del Prete S, Ianniello GP, Micheletto G, Dambrosio M *et al*. (2008). Oxycodone controlled-release as first-choice therapy for moderate-to-severe cancer pain in Italian patients: results of an open-label, multicentre, observational study. Clin Drug Investig 28: 399–407.

Tunblad K, Jonsson EN, Hammarlund-Udenaes M (2003). Morphine blood-brain barrier transport is influenced by probenecid co-administration. Pharm Res 20: 618–623.

Vaughan CW, Ingram SL, Connor MA, Christie MJ (1997). How opioids inhibit GABA-mediated neurotransmission. Nature 390: 611–614.

Watson CP, Babul N (1998). Efficacy of oxycodone in neuropathic pain: a randomized trial in postherpetic neuralgia. Neurology 50: 1837–1841.

Yoshimura M, North RA (1983). Substantia gelatinosa neurons hyperpolarized in vitro by encephalin. Nature 305: 529–530.

Yow TT, Pera E, Absalom N, Heblinski M, Johnston GA, Hanrahan JR *et al*. (2011). Naringin directly activates inwardly rectifying potassium channels at an overlapping binding site to tertiapin-Q. Br J Pharmacol 163: 1017–1033.